

## Small Prototype Aircraft Modelling Using Gvt Test

Vanessa Alvarenga Gomes Cunha<sup>1</sup>, Sérgio Junichi Idehara<sup>1</sup>, Ricardo De Medeiros<sup>2</sup>, Thiago Antonio Fiorentin<sup>1</sup>

<sup>1</sup>(Federal University of Santa Catarina, Mobility Engineering Department, Rua Dona Francisca, 8300 Bloco U, 89.219-600, Joinville, Santa Catarina, Brazil)

<sup>2</sup>(UDESC, Santa Catarina State University, Department of Mechanical Engineering, Rua Paulo Malschitzki, 200, 89.219-710, Joinville, Santa Catarina, Brazil)

Received 12 December 2022; Accepted 26 December 2022

### Abstract:

Vibration is a challenging problem in the process of aircraft design. The expansion of technologies that optimize and reduce the aggregate mass in aeronautical structures or change the traditional material for composite materials may cause structural faults and, thus, require detailed analysis during their development. In this way, experimental modal analysis, in conjunction with finite element methods, has been used to investigate and obtain the necessary dynamic characteristics of the aircraft. The information is applied to predict and quantify possible structural failures. Considering the importance of vibration in aeronautical studies, this work aims to present the ground vibration test (GVT) on an aircraft wing on a small-scale model. The test was performed with an impact hammer, in which four eigenvalues of the wing structure and vibration modes were obtained. For comparison, a finite element model (FEM) was used to model the entire aircraft structure. The obtained undamped modal parameters from that simulation were compared with the experimental results using the natural frequencies as a reference. Which were mostly close to the experimental results (differences of less than 25%). Using the modal assurance criterion (MAC), comparing the mode shapes, we identified three experimental mode shapes correlated with the FEM modes. However, as the frequency increases, the quality of the correlation decreases, due to the system's high damping characteristics.

**Key Word:** Experimental modal analysis; finite element model; aircraft dynamics.

### I. INTRODUCTION

During flying conditions, random vibration acts on aircraft which the engineer considers for the product design. Due to advances in technologies in design tools and products for aeronautical structures, there are innovations with lower mass products. These configurations may have more structural problems that require further analysis of system dynamics [1]. Knowledge of the dynamic response and the behavior of the modifications to aeroelasticity can reduce the occurrence of problems known as buffeting and flutter. These are vibrations in the aircraft structures due to aerodynamic excitations and fluid-structure interaction (unsteady phenomenon), that normally occurs at high air speeds or dynamic pressures. The phenomenon is considered a dangerous condition because it can provoke structure failure in a short period. Furthermore, airplane vibration is a serious problem that is carefully investigated and studied employing computational and experimental tools [2]. Nowadays, experimental modal analysis in combination with finite element methods has been used to investigate and obtain the necessary characteristics of the aircraft for a secure design [3]. Zhang *et al.*[4] explained that for the flight flutter evaluation, it is required to estimate the system modal damping ratio over different flight conditions. One great risk is that the aircraft must fly near the flutter boundary. An aeroelastic model may be constructed, coupling structural motion with fluid dynamic equations to determine the conditions for the flutter events. In this process, the flutter boundary can be estimated numerically [5].

Since understanding the dynamic characteristics of the structures is essential, modal parameters such as natural frequencies, damping factors, and vibrational modes are required. Modal analysis techniques estimate such parameters through analytical, numerical, or experimental approaches. The analytical and numerical forms use the description of a physical model, composed of the matrix of mass, stiffness, and damping. For numerical analysis a software of finite element method (FEM) is used for modeling and predicting the behavior of the structure in addition to seeking improvement in the design [6]. The experimental approach is usually employed to verify and adjust the numerical models [7]. Indeed, [6] and [8] described a traditional Ground Vibration Test (GVT) – where aircraft remain stationary – as a typical and crucial source of data for flutter prediction in the design process. The GVT is also a dynamic structural test requirement for aircraft certification, according to Olejnik&Szczeniak[9]. The test is employed to determine experimentally vibration modes with low frequencies, such as bending and torsion modes of fuselage, wings, tail, and control surfaces (rudder, aileron, and elevator). Song *et al.*[5] showed that the GVT results can be used to obtain a structural model and apply it to

an aerodynamic model to determine the unsteady aerodynamic coefficients. The authors could find the critical flutter value using a reduced-order model as an alternative to traditional calculations.

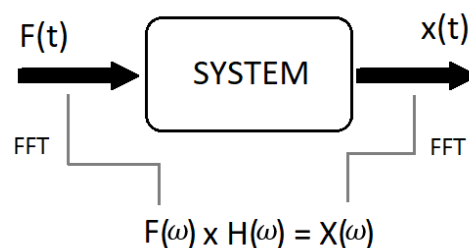
Karaagaçli *et al.*[10] showed that a reliable dynamic analysis is possible only with a good correlation between finite element models and experimental modal results. The authors emphasize the use of model updating methods to construct a representative numerical model. In this way, they developed a methodology to obtain dynamically equivalent models from experimental modal analysis data. In recent years, GVT evaluation has also been performed on an unmanned aerial vehicle (UAV), as it is increasingly used for land mapping, rescuing research [11], agricultural applications, etc. The need for structural analysis is present in this type of vehicle as well. For example, Zuniga *et al.*[12] proposed a UAV model from a ground vibration test for in-flight system identification. That model considers the dynamic characteristics of flexible parts of the UAV, as the common assumption of linearity is limited to 15% of displacement of the wing tip.

Additionally, these works reinforce the importance of FEM models and GVT data for aeronautic applications when the aircraft is being designed and tested. Following this idea, a prototype of a reduced-scale aircraft was used for a GVT experimental test, based on Nisus Aerodesign from the Federal University of Santa Catarina (UFSC). The prototype aircraft was built for the competition of the Society of Automotive Engineers in Brazil. SAE Brazil Aerodesign is an event that allows the development of a detailed real aeronautical product, from conception to the construction and testing phase. As it is a light and flexible aircraft with a simplified internal structure, the used materials may be susceptible to aeroelasticity phenomena and unwanted vibrations, which can interfere with the stability and operational flight envelope [7]. This work presents the modal analysis of the wing of that small prototype, evaluated numerically through the finite element model and the GVT. The last is used as a verification target for the simulation results.

### MODAL ANALYSIS

The vibration characteristic of a structure is determined by the material property and geometry (mass, stiffness, and damping), and by the boundary conditions. The experimental modal analysis is a simple and efficient way of measuring and characterizing natural modes of vibration. This area phenomenon caused by the interaction between the inertial and elastic properties of the material and the structure. Vibration modes are usually the cause or, at least, one factor that contributes to problems involving structures and machines in operation [13]. Therefore, to understand and measure structural vibration, the resonance frequencies should be identified, generally, through simulations and experimental tests. Experimental evaluation has been used since the early 1970s, with the advent of the Fourier Fast Transform techniques (FFT), concomitantly with impact tests. That is a fast and economical way to find the vibration modes of a structure according to [13]. The experimental modal parameters may be determined by the Frequency Response Function (FRF), which relates the system response signal  $x(t)$  with the force in the input signal  $F(t)$ . The illustration in Figure 1 shows the block diagram and the calculation of FRF from the spectrum of the measured time response and force signal.

**Figure 1:** Block diagram illustration of the system dynamic.



According to [7], experimental modal analysis is a fundamental technique used to estimate the vibrational parameters of a complex structure, which aims to validate and improve finite element modeling. In this way, the Ground Vibration Test (GVT) is a standard experimental test widely used in the final stages of development. The extraction of modal parameters from the data measured during the test is a post-processing step that can be performed using parameter identification techniques, based on the time or frequency response of the system. There are various different methods, such as the autoregressive moving-average (ARMA) method, least-squares complex exponential method (LSCE), polyreference complex exponential method (PRCE), global rational fraction polynomial (GRFP), etc., indicated by Maia and Silva [14]. Other forms of modal analysis, in increasing demand from engineering, are operational modal analysis (OMA) and impact synchronous modal analysis (ISMA), as presented by Zahid, Ong, and Khoo[15]. Some techniques based on digital image correlation are also employed to develop modal analysis results [16]. In this study, an established experimental

modal analysis (EMA) was used in a laboratory environment with a polyreference method as the parameter estimator.

The damping in the mathematical modeling is related to the system's internal energy dissipation, which attenuates the vibration amplitude (in free vibration response). Also, it affects the natural frequencies (eigenvalues) and vibration modes (eigenvectors) of the system. One of the most common damping models for analysis is viscous, structural, Coulomb (dry friction), and hysteretic damping. Eq. (1) gives a generalized equation of motion for the structural damping model in a multiple-degree-of-freedom system, as presented by [17],

$$[M].\{\ddot{x}\} + i.[C].\{\dot{x}\} + [K].\{x\} = \{F\} \quad (1)$$

where,  $[M]$ ,  $[C]$ , and  $[K]$  are  $(n \times n)$  dimensional matrices of mass, damping, and stiffness, respectively.  $n$  is the system degree of freedom. The variables  $\{\ddot{x}\}$ ,  $\{\dot{x}\}$ ,  $\{x\}$  and  $\{F\}$  are  $(n \times 1)$  vectors of acceleration, velocity, displacement, and force, respectively. Adopting a solution to Eq. (1), the vector  $\{x(t)\} = \{X\}e^{\lambda t}$ , where  $\{X\}$  is the displacement vector,  $\lambda$  corresponds to the eigenvalue, and  $t$  is the time variable, we obtain the eigenvalues and eigenvectors associated with the system. The eigenvalue takes the form of  $\lambda_r = \pm\omega_r \cdot \sqrt{(1 + \eta_r)}$ , where  $\omega_r$  corresponds to the natural frequency and  $\eta_r$  the structural damping loss factor, which depends on the material property.

The FRF data may be determined by a receptance matrix, based on the harmonic input force in the system, expressed in Eq. (2). The Eq(3) and Eq. (4) show normalized modes from the mass matrix and system eigenvector,

$$\{X(\omega)\} = ([K] + i[C] - \omega^2[M])^{-1} \cdot \{F\} = [\alpha(\omega)] \cdot \{F(\omega)\} \quad (2)$$

$$\{X\}_r^T [M] \{X\}_r = m_r, r = 1, \dots, n \quad (3)$$

$$\{\Phi\}_r = \frac{\{X\}_r}{\sqrt{m_r}}, r = 1, \dots, n \quad (4)$$

By multiplying Eq. (2) with the transposed modal matrix normalized by the mass  $[\Phi]$ , it was obtained:

$$[\Phi]^T ([K] + i[C] - \omega^2[M])[\Phi] = [\Phi]^T [\alpha(\omega)]^{-1} [\Phi] \quad (5)$$

Equation (5) determines the receptance matrix, relating the input and output parameters of a linear discrete mechanical system that is subjected to harmonic force. The receptance matrix is rewritten as:

$$[\alpha(\omega)] = \frac{[\Phi] \cdot [\Phi]^T}{[diag(\lambda_r - \omega^2)]} \quad (6)$$

The matrix of the frequency response function of  $[\alpha(\omega)]$  contains the symmetry property and the reciprocity principle, so that  $\alpha_{jk} = \alpha_{kj}$ . Therefore, Eq.(7) indicates the vectors of each FRF[18], as

$$\alpha_{jk}(\omega) = \frac{X_j}{F_k} = \sum_{r=1}^N \frac{\phi_{jr} \cdot \phi_{kr}}{\omega_r^2 - \omega^2 + i\eta_r \cdot \omega_r^2} \quad (7)$$

The parameter  $\omega_r$  is the system's natural frequencies resulting from the eigenvalues.

By Eq.(7) the response of a system with  $n$  degrees of freedom can be seen as the sum of the individual responses of each vibration mode. Thus, the methods for estimating modal parameters in frequency use this mathematical expression as a basis to obtain the estimation of the eigenvalues and eigenvectors. The estimator used in this work belongs to the group of estimators of the frequency method.

## II. MATERIAL AND METHODS

### EXPERIMENTAL AIRCRAFT PROTOTYPE

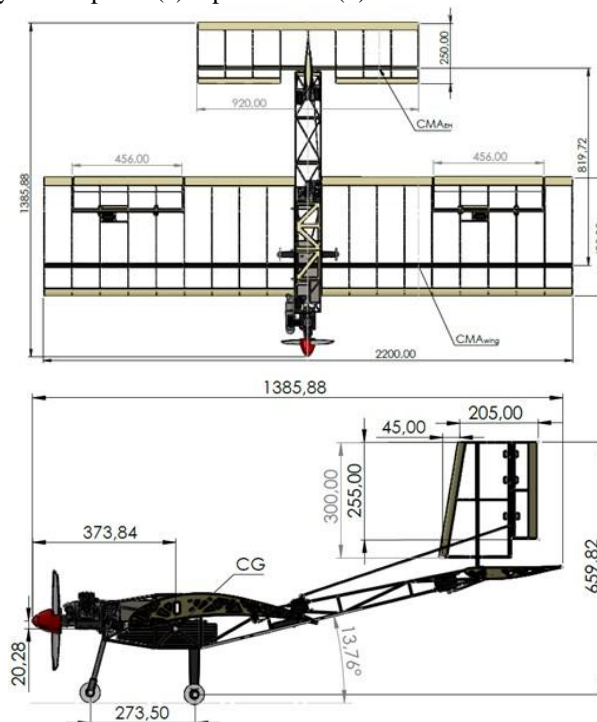
The aircraft used in the present study was from the Nisus Aerodesign team (UFSC/ Joinville) presented in Figure 2. The prototype was used in the SAE BRASIL competition in 2019. The aircraft dimensions are presented in Figure 3; (a) top view and (b) side view. The fuselage is 1090 mm long and 105 mm wide and was built with joined fiberglass rods using epoxy resin. The firewall and floor base were made in a sandwich structure, with an aramid honeycomb core and two faces of fiberglass fabric laminated with epoxy resin, with thicknesses of 3.1 and 3.2 mm respectively.

The wing of the aircraft has a rectangular shape with a chord equal to 490 mm and a wingspan of 22,000 mm. It consists of a 1 mm thick hollow rectangular section spar, laminated with carbon fiber impregnated with epoxy resin, and two 3 mm diameter glass fiber reinforcement spars as shown in Figure 3. Also, it is mounted with two central ribs, made of composite material of carbon fiber, and 3.5 mm thick landing gear. The other parts of the wing had 18 balsa wood ribs with a thickness of 2 mm, and for the leading and trailing edges, the balsa wood sheets were 1.79 and 1.5 mm respectively.

Figure 2: Prototype of the airplane from Nisus Aerodesign.



Figure 3: Capybara airplane (a) top view and (b) side view. Dimensions in millimeters.



**FINITE ELEMENT MODEL**

Finite element analysis/ method (FEA or FEM) is a well-known numerical technique for determining the dynamic characteristics of mechanical systems [19]. However, the results obtained by FEM are often subject to errors due to modeling errors or incorrect boundary conditions [20]. The finite element methodology is illustrated in the flowchart in Figure 4. Some steps may be suppressed according to the modeling requirements. In general, the model is generated based on CAD design, the definition of material properties with subsequent discretization by a mesh, and the definition of boundary conditions. Followed by the execution of the numerical processing to obtain the results and finished with post-processing to visualize the information. The FEM model for this work was created in Ansys® 16 as illustrated in Figure 5. The longitudinal direction is oriented along the x-axis, the transversal direction is the z-axis, and the vertical direction is on the y-axis. The last one is employed as a reference for the accelerometer measurements.

The materials used in the simulation were based on fiberglass and balsa wood properties from online material property data (www.matweb.com). The value of the properties is presented in Table 1. The different properties according to fiber orientation and contact with the epoxy matrix were not taken into account in this analysis, and it may differ some natural frequencies and vibration modes from the experimental results.

**Figure 4:** Flowchart of finite element method.

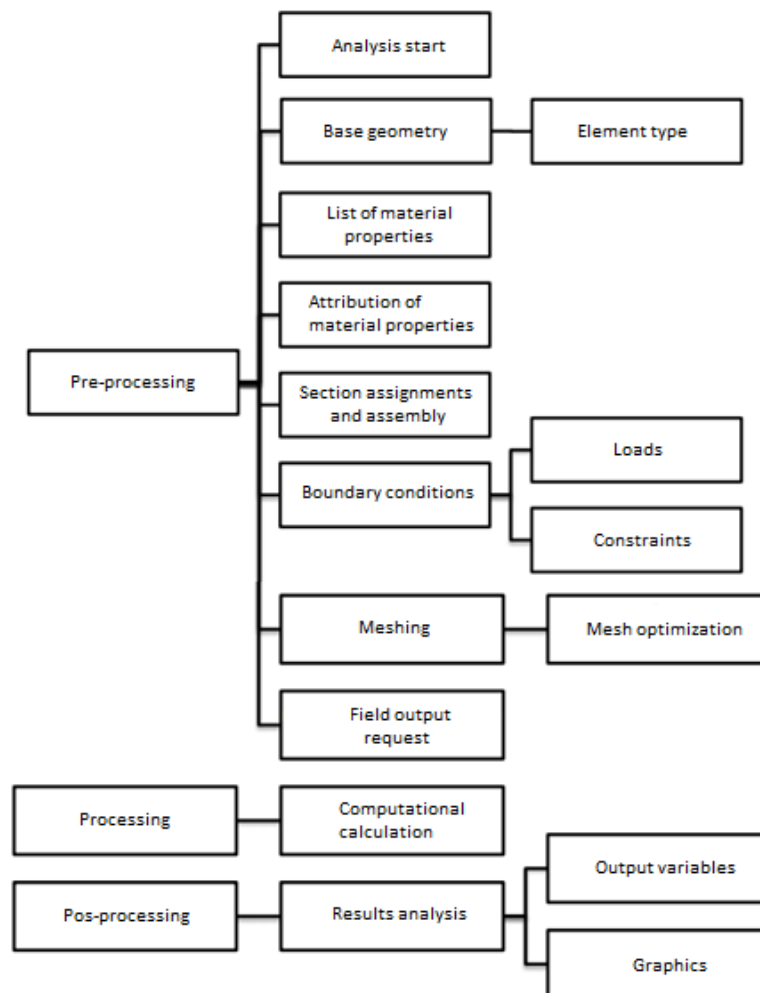


Figure 5: Element Finite model in Ansys® software.

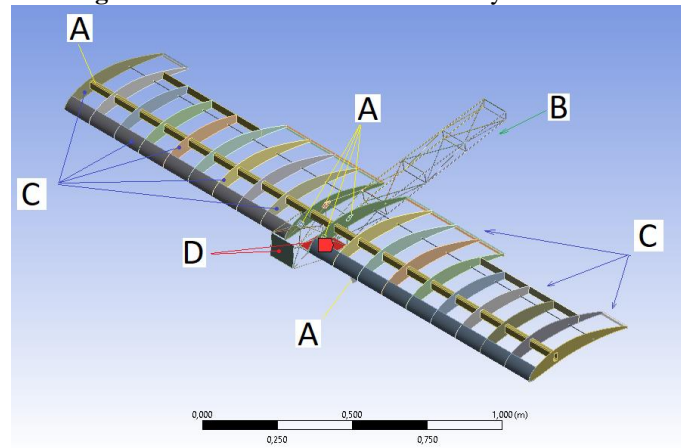


Table 1: FEA model properties.

	Material	Elastic Modulus [GPa]	Poisson Coefficient [-]	Density [g/cm <sup>3</sup> ]
A	Fiber Glass (wing)	70.0	0.29	1.41
B	Fiber Glass (fuselage)	1.0	0.30	2.00
C	Balsa wood (wing/ landing gear)	0.6	0.38	0.60
D	Fiber Glass (floor and nose)	35.0	0.28	1.85

### EXPERIMENTAL MODAL ANALYSIS

The wing surface, along the vertical axis (y-axis), was chosen as the target mode to be analyzed. Following Pickrel[21] methodology for the experimental modal test, an impact excitation was conducted for different points along the wing length and width. The response acceleration was measured as a constant position as indicated at point 9 of Figure 6. The number of measured points on the wing is according to a rule from [21], which for the mode shapes definition is applied:

$$N_{sensor} > 10. N_{modes} \quad (8)$$

where the  $N_{sensor} = 60$  is the number of measured points and  $N_{modes} = 4$  the number of estimated modes for visual and quantitative analysis in this work.

According to Jafri [20], the initial adjustment of the model must be made from the determination of the degree of correspondence between the experimental and analytical models. Since a good correlation is crucial for the success of the model update, the comparison between the experimental and numerical natural frequencies is presented in the results, observing the differences between the two values. In addition to natural frequency comparison, another way to achieve model correlation is by comparing vibration modes. To compare the modal modes, the deflected shapes of the structure are plotted for a particular mode, using both experimental data and a numerical model. These graphic modal shapes may give a quick comparison and an idea of the model's correlation with the real structure [20]. In addition, as a quantitative analysis calculation, the Modal Assurance Criterion (MAC) makes the correlation between the experimental and numerical modes as defined by Pastor, Binda, and Harcarik [22]. The sub-indices  $r$  and  $s$  represent experimental and numerical modes to be compared:

$$MAC_{r,s} = \frac{|\{\phi_r\}^T \cdot \{\phi_s^*\}|^2}{\{\phi_r\}^T \cdot \{\phi_r^*\} \cdot \{\phi_s\}^T \cdot \{\phi_s^*\}} \quad (9)$$

The experimental test of the modal analysis in the Nisus Aerodesign aircraft (Figure 7) was carried out using the acquisition data system from Brüel&Kjaer (Pulse Lab Shop, version 16.1.1) at the Vibration and Lightweight Structure Laboratory (LaVEL) of Santa Catarina State University (UDESC). An impact hammer was instrumented with a force transducer applied as input to the mechanical system, and an accelerometer type 4397 as the system output signal. The information about instrumentation is presented in Table 2. The impact input signal was repeated three times per point for the averaging processing.



Figure 6: Excited points from the wing test of the Nisus Aerodesign aircraft (from 1 to 60). Highlighted the measured point at point 9.

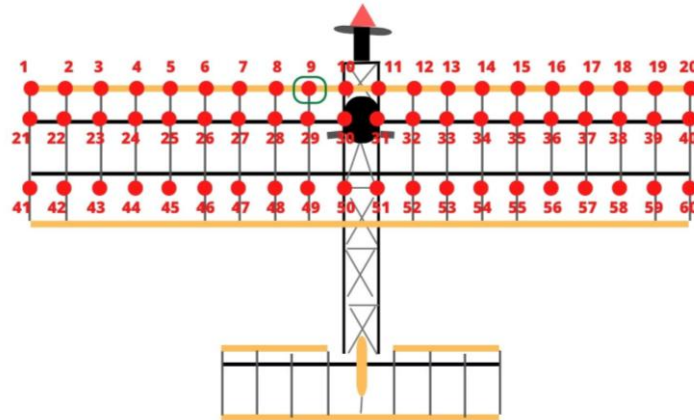


Figure 7: Modal analysis setup of the Nisus aircraft prototype.

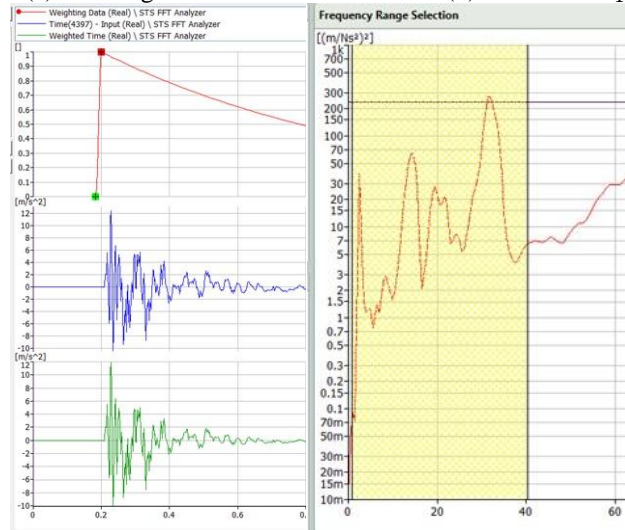


Table 2: Instrumentation datasheet information.

	Impact hammer load cell BK 8206-003	Accelerometer BK DeltaTron 4397
Serial Number	56310	31317
Sensitivity	1.12mV/N	1.00mV/ms <sup>2</sup>
Range	Max. 4448.00N	1.00Hz to 25.00kHz

The signal acquisition module on the modal analysis setup was configured for a sample rate of 51.2 kHz. For the post-processing of measured signals, the frequency range of the FRF was from zero to 200 Hz with 400 lines (interval of 0.5 Hz for 2.0 s of measurement and three samples). The type of window used in the temporal response of the measured accelerometer was the exponential window. The weighting window function is applied to reduce errors due to leakage phenomena, as shown in Figure 8(a). The measured data was processed using Reflex software with  $H_1$  estimator for the FRF Figure 8(b), which is the result of a cross-spectrum between the output and input signals divided by the input spectrum. The Polyreference method with 128 iterations was applied to estimate the modal parameters within a frequency range between 1.0 Hz and 40.0 Hz.

Figure 8: (a) Time signal from measurement and (b) FRF from  $H_1$  response.



### III. RESULTS

#### GVT TEST

From the modal algorithm estimator, four vibration modes were identified at frequencies of 2.36Hz, 14.15Hz, 22.64Hz, and 31.95Hz. The mode shapes are shown in Figure 9. For frequencies higher than 40Hz, the FRF becomes more attenuated by the damping level of the structure, making it difficult to estimate the modal parameters. Table 3 shows the damped natural frequencies and the corresponding damping factors.

Figure 9: Identified modes from the Polyreference method.

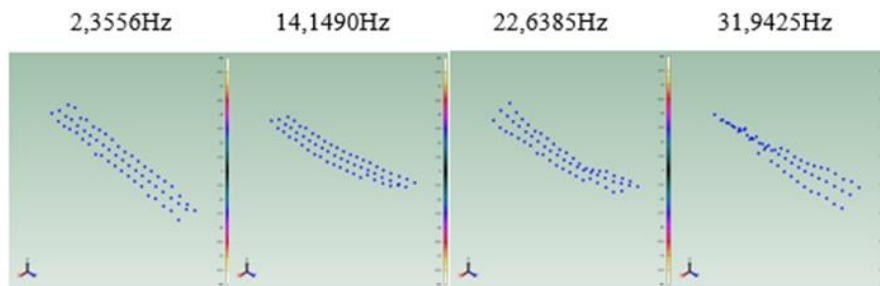


Table 3: Experimental damped natural frequencies and damping factor.

Modes	Natural frequency [Hz]	Damping factor [%]
1	2.36	10.07
2	14.15	7.94
3	22.64	10.50
4	31.94	4.03

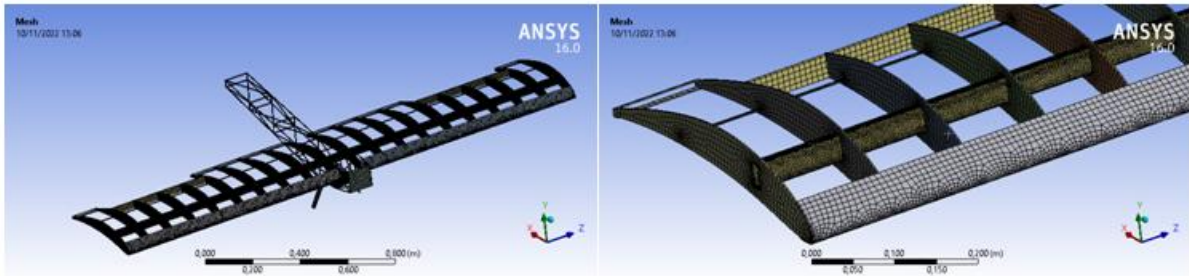
#### COMPARISON BETWEEN FEM AND MODAL ANALYSIS

The finite element of the wing-fuselage set was employed to verify the numerical modes and natural frequencies and compare the results from the experimental modal analysis. Based on the configuration of the experimental setup, a mass of 1.56kg was added to the surface of the aircraft floor model to regulate the position of the center of gravity (Figure 5). In the experiment, this mass simulated the engine weight and made it possible to keep the aircraft in the horizontal position, as shown in Figure 7. The structural components of the FEM model were associated with the material based on Table 1, and the contacts were manually configured between the wing components and joints along the volume edges and faces as a bounded contact. The mesh convergence analysis was performed. The process of mesh convergence involves decreasing the element size and analyzing the impact of this process on the accuracy of the solution. Thus, the numerical model had 363,262 nodes and



178,560 elements as illustrated by Figure 10(a). An amplified view of the wing is presented in Figure 10(b) The 20 first modes were calculated between 1.5 and 40.0Hz.

**Figure 10:** Finite element model of (a) Nisus prototype and (b) zooming of the wing.



The natural frequencies of the FEM model and those obtained in the experimental modal analysis, which correlated to y-axis vibration, are presented in Figure 11. In this case, just the wing vibration modes are compared. It can be seen that the frequencies of the first two numerical modes are higher than the experimental ones, and lower for the last two modes. This indicates that an adjustment of the model may improve the correlations between this numeric and the real system. One factor that would significantly influence the accuracy of natural frequencies is the properties of the materials. Since they were composite materials and the properties are variable depending on the manufacturing process, the values applied in the model may not be close to the tested aircraft.

The modes of vibration obtained in the simulation are presented in Figure 12. These modes are vibration on the prototype wing, such as a wing rigid rotation, first bending, torsion, and second bending, respectively first to the fourth mode.

The quantitative correlation of the numerical and experimental modes from the MAC matrix is presented in Table 4, in which the lines represent the experimental modes and the columns the numerical modes. There is a good correlation (MAC around 90%) of mode 1 of the experimental (2.37 Hz) with numerical mode 1 (7.80 Hz). Experimental mode 2 (14.19 Hz) and mode 3 (22.76 Hz) present some correlation with numerical mode 2 (17.09 Hz) and 3 (19.83 Hz), respectively, with MAC around 50%. However, the fourth experimental mode (31.97 Hz) does not show any strong correlation with any specific numerical mode from the MAC correlation, as they were below 40%. When analyzed visually, the closest mode appears to be the numerical fourth mode. The decreasing correlation between vibration modes in higher frequency modes may be caused by high damping values of the structure, which lower the quality of estimation.

**Figure 11:** Comparison between undamped natural frequencies (EMA vs. FEM).

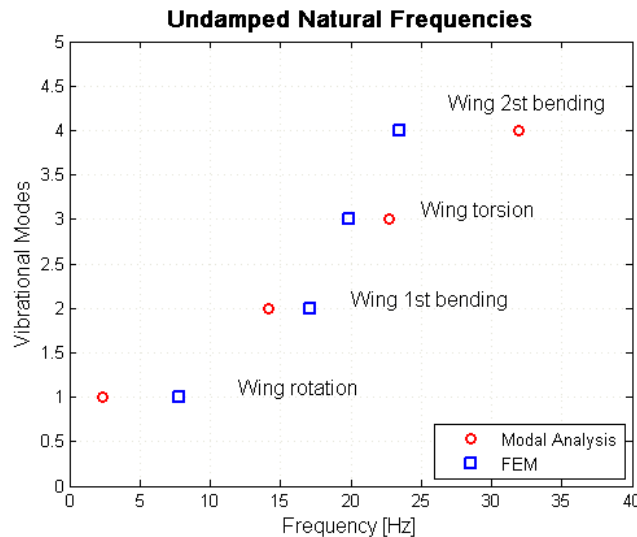
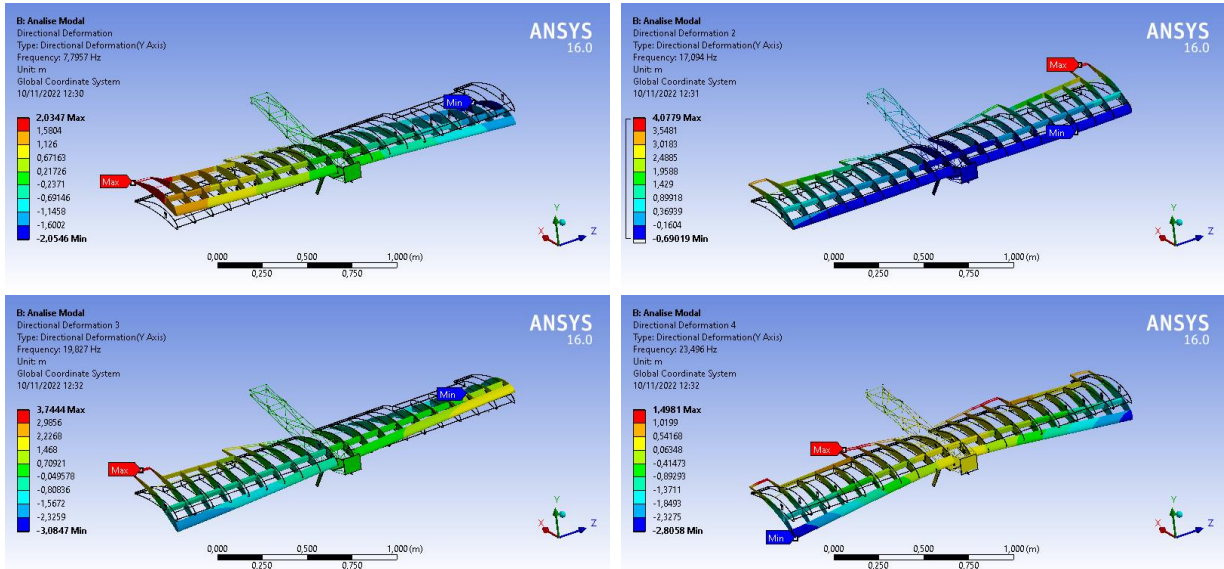


**Figure 12:** Vibration modes from FEM modeling (a) wing rotation, (b) wing first bending, (c) wing torsion and (d) wing second bending mode.



Thus, although the natural frequencies of the finite element model are not obtained through the same method used in the experimental modal analysis (GVT), there are similarities between the first modes in the way the nodes vibrate that resemble the way the real wing vibrates. Therefore, it can indicate that the model built is somehow representative of the real system. However, it requires adjustment in its parameters so that the natural frequencies and vibration shape are also coincident. The main reason for differences between the experimental and numerical modes are the material properties values that were not measured before entry into the simulation.

**Table 4:** MAC comparison between numerical and experimental modes.

Experimental	Numerical				
	[Hz]	7.80	17.09	19.83	23.50
2.37	90.08	0.43	1.13	0.41	
14.19	9.35	48.97	1.40	20.20	
22.76	15.71	13.51	43.38	1.07	
31.97	32.61	12.38	3.69	23.16	

#### IV. CONCLUSION

In this study, a GVT (ground vibration test) and numerical modeling of a small prototype aircraft wing were performed, which characterized its structural dynamic behavior. The experimental tests on the wing were based on standard modal analysis techniques with impact excitation. During the tests, four modes were identified between 1.5 and 50Hz. Higher frequency modes are too damped to be determined. The numerical model in the finite element method discretized the entire airplane and the wing-undamped vibration modes were identified. Between the comparison of the experimental and numerical results, the difference in the natural frequencies was less than 26% relative to the experimental data for the last three modes. In the first mode, for a rigid rotation of the wing, the difference in the natural frequency was higher. The type of used contact model between wing and fuselage, as bounded, may give a higher frequency in the numerical model, whereas in the real aircraft there could be less stiffness. In the comparative analysis of the mode shapes, the MAC value indicated a better correlation between experimental and numerical modes for the first modes. Conversely, for the higher natural frequency modes, the MAC value decreases. The results obtained show that due to the difficulties in measuring a material that was highly lighted and damped, it was difficult to estimate the modes with higher natural frequencies.

#### REFERENCES

- [1]. Demirtas A, Bayraktar M. Free vibration analysis of an aircraft wing by considering as a cantilever beam. *Sujest.* 2019;7(1):12–21.
- [2]. Sommer T, et al. The pilot influence on the flutter velocity of the lightweight plane. *METEC WEB Conferences.* 2019.

- [3]. Salgado J, Meireles J. Study of the experimental modal analysis techniques applied to structural dynamics. In: 5th International Operational Modal Analysis Conference. Guimarães, Portugal, 2013;131.
- [4]. Zhang W, Lv Z, Diwu Q, Zhong H. A flutter prediction method with low cost and low risk from test data. *Aerospace Science and Technology*. 2019;86:542–557.
- [5]. Song J, Kim T, Song SJ. Experimental determination of unsteady aerodynamic coefficients and flutter behavior of a rigid wing. *Journal of Fluids and Structures*. 2012;29:50–61.
- [6]. Hernández S, Menga E, Moledo S, Romera LE, Baldomir A, López C, Montoya MC. Optimization approach for identification of dynamic parameters of localized joints of aircraft assembled structures. *Aerospace Science and Technology*. 2017;69:538–549
- [7]. Gasparetto VEL, Machado MR, Carneiro SHS. Experimental modal analysis of an aircraft wing prototype for SAE Aerodesign Competition. *Revista DYNA*. 2020;87(214):100-110.
- [8]. Chajec W. Flutter calculation based on GVT-results and theoretical mass model. *Aviation*. 2009;13(4):122–129.
- [9]. Olejnik A, Kachel S, Rogólski R, Szczesniak M. Technology of Ground Vibration Testing and its application in light aircraft prototyping. *MATEC Web of Conferences*. 2019;304:1–8.
- [10]. Karaagaçlı T, Yıldız EN, Ozguven HN. New method to determine dynamically equivalent finite element models of aircraft structures from modal test data. *Mechanical Systems and Signal Processing*. 2012;31:94–108.
- [11]. Pellegrini CC, Rodrigues MS, Moreira EO. The development of an educational software for aircraft flight mechanics calculations. *Physics Education paper*. 2021:1–12.
- [12]. Zúñiga DFC, Souza AG, Góes LCS. Flight dynamics modeling of a flexible wing unmanned aerial vehicle. *Mechanical Systems and Signal Processing*. 2020;145:1–16.
- [13]. Schwarz B, Richardson M. Experimental modal analysis. *CSI Reability Week*. Orlando, 1999.
- [14]. Maia NMM, Silva JMM. Modal analysis identification techniques. *Phil. Trans. R. Soc. Lond. A*. 2001;359:29–40.
- [15]. Zahid FB, Ong ZC, Khoo SY. A review of operational modal analysis techniques for in- service modal identification. *Journal of the Brazilian Society of Mechanical Sciences and Engineering*. 2020;42(398):1-18.
- [16]. Frankovsky P, Delyová I, Sivák P, Bocko J, Zivcak J, Kicko M. Modal Analysis Using Digital Image Correlation Technique. *Materials*. 2022;15:1-15.
- [17]. Ewins DJ. *Modal Testing: Theory, Practice and Application*. Wiley, 2<sup>nd</sup> Edition, 2009. ISBN 978-0-863-80218-8.
- [18]. Maia NMM. *Theoretical and Experimental Modal Analysis*. Research Studies Pre, 1997. ISBN 978-0863802089.
- [19]. Aabid A, Zakuan MAMB, Khan SA, Ibrahim YE. Structural analysis of three-dimensional wings using finite element method. *Aerospace Systems*. 2022;5:47–63.
- [20]. Jafri H, Mohammad A. Finite element modeling and its validation using experimental modal analysis. *International Journal of Scientific & Engineering Research*, 2016.
- [21]. Pickrel CR. A practical approach to modal pretest design. *Mechanical Systems and Signal Processing*. 1999;13(2):271–295.
- [22]. Pastor M, Binda M, Harcarik T. Modal assurance criterion. *Procedia Engineering*. 2012; 48:543–548.

Vanessa Alvarenga Gomes Cunha, et. al. "Small Prototype Aircraft Modelling Using Gvt Test." *IOSR Journal of Engineering (IOSRJEN)*, 12(12), 2022, pp. 11-21.